S.H.MAMMADOVA
F.M.SADIQOV
saba.mammadova36@gmail.com
Baku State University

UOT: 544.31:546.666'23/24

THE PHASEFORMATION IN THE Ce_2Se_3-Sb_2Se_3-Bi_2Se_3 QUASI-TERNARY SYSTEM

Based on the literature data, as well as the results obtained by the methods of physicochemical analysis, the character of phase formation in the Ce_2Se_3-Sb_2Se_3-Bi_2Se_3 quasi-ternary system was determined. The phase diagrams of a number of internal sections (Sb_2Se_3-$CeBiSe_3$, Ce_2Se_3-$CeSb_{1,5}Bi_{1,5}Se_6$, Bi_2Se_3-$CeSb_{1,5}Bi_{1,5}Se_6$, $CeSbSe_3$-$CeBiSe_3$), the isothermal section at 300 K, and the projection of the liquidus surface were constructed, the types and coordinates of non- and monovariant equilibria were obtained. The existence of six ternary compounds, $S_1(Ce_8Sb_2Se_{15})$, $S_2(Ce_6Sb_4Se_{15})$, $S_3(CeSbSe_3)$, S_4 $(CeBiSe_3)$, S_5($CeSb_{1,5}Bi_{1,5}Se_6$) and S_6 $(Ce_8Bi_2Se_{13})$, as well as regions of solid solutions based on the initial Sb_2Se_3 , Bi_2Se_3 , as well as S5 compounds was shown.

Key words: *Antimony and bismuth chalcogenides, REE chalcogenides, quasi-binary section, non-quasi-binary section, liquidus surface projections*

1. Introduction.

Antimony and bismuth selenides are promising materials with a narrow band gap and a high absorption coefficient. Due to these features, they are important materials for optoelectronic applications [1, s.2], solar cells [3], thermoelectric converters [4-7], photoelectrochemical cells [8], optical recording [9], lithium-ion batteries [10, 11]. Moreover, they are also used as a topological insulator [12-14] and superconductors [15].

The introduction of atoms of rare earth elements (RFE) into the crystal structure of these compounds can lead to an improvement in these properties.

The results of physicochemical interaction in the Ln_2X_3-Sb_2X_3- Bi_2X_3 (Ln-REE; X-S, Se, Te) systems are presented in a number works [16-26].

The purpose of present work is to study phase formation in the Ce_2Se_3-Sb_2Se_3-Bi_2Se_3 quasi-ternary system.

Previously, the ternary systems Ce-Sb-Se and Ce-Bi-Se were studied along the Sb_2Se_3-Ce_2Se_3 and Bi_2Se_3-Ce_2Se_3 sections [18, s.19]. Ce_2Se_3 compound melts at 1970 K and crystallizes in a cubic singony [18, 19]. Sb_2Se_3 and Bi_2Se_3 melt at 863 and 979 K, accordingly [18, s.19]

The Sb_2Se_3-Bi_2Se_3 boundary system is characterized by the formation of continuous solid solutions.

The ternary systems Ce-Sb-Se and Ce-Bi-Se are characterized by formation of the $CeSbSe_3$ $Ce_6Sb_3Se_{15}$, $Ce_8Sb_2Se_{15}$, $CeBiSe_3$ and $Ce_8Bi_2Se_{15}$ ternary compounds [18, s.19].

2. Experimental part.

2.1. Materials and Synthesis.

The starting materials for the synthesis of initial compounds and intermediate alloys were high-purity elements cerium (7440-45-1), bismuth (7440-69-9), arsenic (7440-36-0), selenium (7782-49-2), purchased from by Alfa Aesar.

The alloys were obtained by direct alloying of the components in quartz ampoules at 1000–1200 K (depending on the composition) followed by slow cooling in the off-furnace rejime.

To obtain an equilibrium state, the alloys were subjected to homogenizing annealing at temperatures 50–100 K below the solidus temperature for two weeks.

2.2. Research methods.

The studies were carried out by a set of methods of physicochemical analysis, namely, differential thermal (DTA), X-ray diffraction (XRD), microstructural (MSA) methods and measurement of microhardness and density.

The heating curves of thoroughly homogenized alloys were recorded on a BDTA-8M2 pyrometer in an inert atmosphere using W-W/Re thermocouples, heating rate 40 K/min, temperature determination accuracy ±10 K while for NTR-73 pyrometer was 10 K/min, temperature determination accuracy ±5K. All observed effects were endothermic and reversible.

XRD was performed on a Bruker D8 diffractometer (CuK_α- radiation).

MSA was performed on MBI-6 and MIM-7 microscopes. In the study of the microstructure of the alloys, an etchant with the composition of 10 ml of concentrated H_2SO_4 + 5 g $K_2Cr_2O_7$ + 90 ml H_2O.

The microhardness was measured on a PMT-3 microhardness meter at an optimally chosen load of 10, 20, and 30 g. depending on composition.

3. Results and discussion.

Based on the data obtained by the above methods, the phase diagrams of the Sb_2Se_3-$CeBiSe_3$, Ce_2Se_3-$CeSb_{1,5}Bi_{1,5}Se_6$, Bi_2Se_3-$CeSb_{1,5}Bi_{1,5}Se_6$, $CeSbSe_3$ - $CeBiSe_3$ systems were constructed.

In the article the following designations of compounds are adopted $S_1(Ce_8Sb_2Se_{15})$, $S_2(Ce_6Sb_4Se_{15})$, $S_3(CeSbSe_3)$, S_4 $(CeBiSe_3)$, S_5($CeSb_{1,5}Bi_{1,5}Se_6$) and S_6 $(Ce_8Bi_2Se_{13})$.

The **Sb_2Se_3-$CeBiSe_3$** section (Fig. 1) is quasi-binary, belongs to the eutectic type. When the ratio of the starting compounds is 1:1, the $CeSb_{1,5}Bi_{1,5}Se_6$ quaternary compound with congruently melting at 1050 K is formed. This compound forms a eutectic with $CeBiSe_3$ (the eutectic coordinates are 25 mol.% Sb_2Se_3, 700 K) and with an α-solid solution based on Sb_2Se_3 (25 mol.% $CeBiSe_3$, 600 K). Regions of solid solutions were found in the system near Sb_2Se_3 up to approximately 5 mol.%, and based on $CeBiSe_3$ up to 3 mol.% at room temperature. A region of solid solutions near $CeSb_{1,5}Bi_{1,5}Se_6$ was also found up to approximately 2 mol.% Sb_2Se_3 and 1.5 mol.% $CeBiSe_3$ at 300K.

Based on powder XRD data, it was found that the $CeSb_{1,5}Bi_{1,5}Se_6$ compound crystallizes in a rombic lattice with unit cell parameters *a*=1.625; *b*=2.392; *c*=0.404 nm

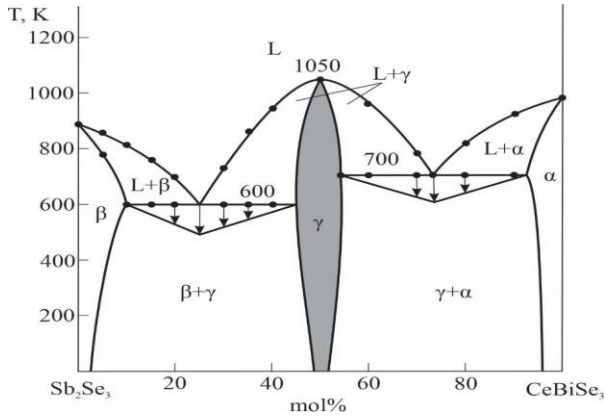

Fig.1. *Phase diagram of the Sb_2Se_3- $CeBiSe_3$system*

The section Ce_2Se_3-S_5($CeSb_{1,5}Bi_{1,5}Se_6$) is quasi-binary (Fig. 2), eutectic type. The eutectic

corresponds to the composition of 50 mol.% S5 and 800K. Solubility based on S_5 at 300 K reaches 2 mol.% Ce_2Se_3. Solubility based on Ce_2Se_3 is practically not detected.

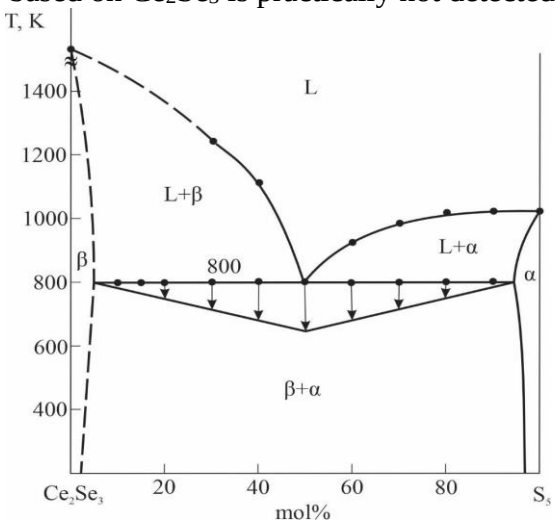

Fig.2. *Phase diagram of the Ce_2Se_3- S_5 system*

The Bi_2Se_3-S_5 section is also quasi-binary (Fig. 3), belongs to a simple eutectic type, eutectic coordinates: 70 mol.% S_5 and 900K. The area of solid solutions based on the Bi_2Se_3 at 300 K reaches 10 mol.% S_5 and based on S_5 up to 5 mol.% Bi_2Se_3.

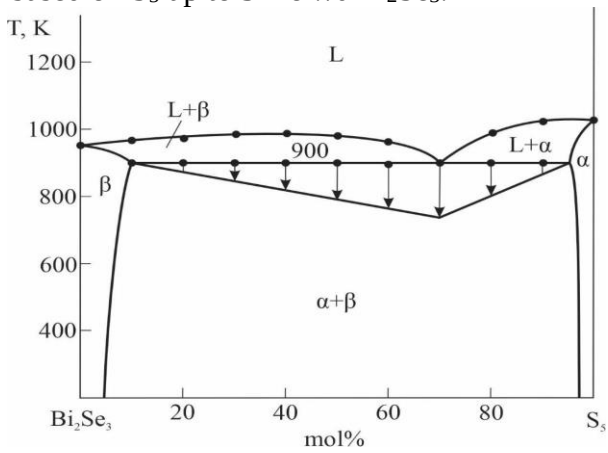

Fig.3. *Phase diagram of the Bi_2Se_3- S_5 system*

The S_2-S_4 section (Fig. 4) is non-quasi-binary, crosses two subordinate triangles of the Sb_2Se_3- Ce_2Se_3- S_5 and Ce_2Se_3- S_5- S_4 ternary system.

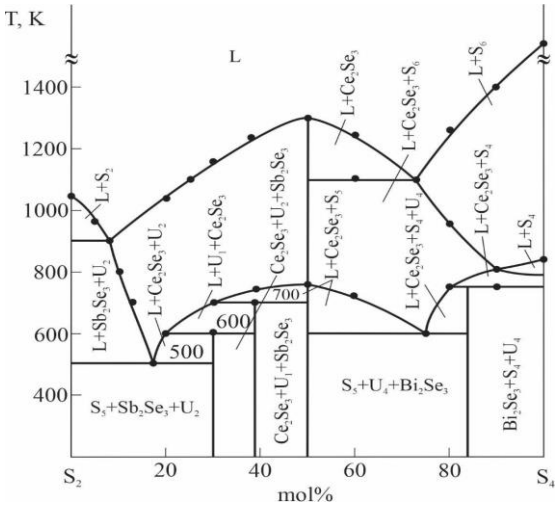

Fig.4. *Phase diagram of the S_2- S_4 system*

The liquidus curve of this section consists of three curves of primary phase crystallization: $S_6(Ce_8Bi_2Se_{15})$,Ce_2Se_3 and $S_2(Ce_6Sb_4Se_{15})$. All alloys of subordinate triangles complete crystallization in ternary eutectics:

I. ж↔ $S_5 + Sb_2Se_3 + U_2(CeSbSe_3)$ (500K)

II. ж↔ $S_5 + U_4(CeBiSe_3) + Ce_2Se_3$ (600K)

Part of the system crosses particular triangles I and II, where the following peritectic transformations take place:

ж+ Ce_2Se_3 ↔ $S_1(Ce_8Sb_2Se_{15}) + S_5$ (700K)

ж+ Ce_2Se_3 ↔ $S_3(CeSbSe_3) + S_5$ (600K)

ж+ Ce_2Se_3 ↔ $S_6(Ce_8Bi_2Se_{15}) + S_4$ (780K)

The S_3-S_4 section (Fig. 5) is non-quasi-binary, crosses the S_5–S_4-Bi_2Se_3 subordinate triangle, where

ж↔ $Bi_2Se_3 + S_5 + S_4$ (700K)

ж+ S_6 ↔ $S_4 + S_5$ (800K)

eutectic and peritectic transformations occur:

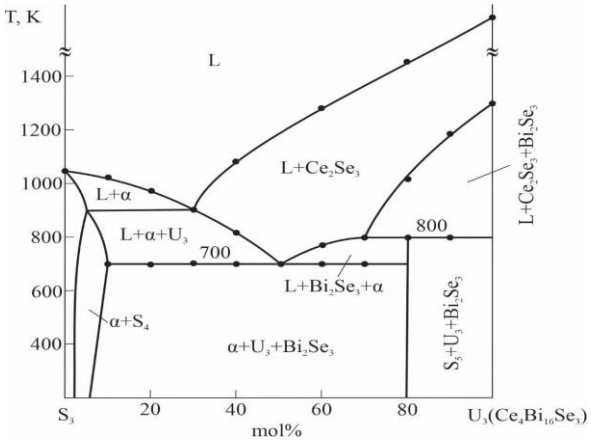

Fig.5. *Phase diagram of the S_3-S_4 system*

Liquidus consists of three curves of the primary crystallization of the Ce_2Se_3 , S_5 and $\alpha(S_5)$-phases. Solubility based on S_5 is 3 mol.% at 300K.

The projection of the liquidus surface of the Ce_2Se_3-Sb_2Se_3-Bi_2Se_3 ternary system was constructed based on the literature data on binary systems [27, 28] and experimental data of three quasi-binary and two non-quasi-binary sections (Fig. 6).

The Ce_2Se_3-Sb_2Se_3-Bi_2Se_3 system is triangulated into four subordinate ternary systems: Sb_2Se_3- S_5- Ce_2Se_3, Sb_2Se_3- S_5- Bi_2Se_3, Ce_2Se_3- S_5- S_4 and S_5- S_4.

8 fields of primary crystallization of initial components are defined in the system. The most extensive area is the field of crystallization of the S_5 phase, and the smallest is the field of crystallization of the S_4 phase.

The Ce_2Se_3-Sb_2Se_3-Bi_2Se_3 system is characterized by the presence of 8 invariant eutectic (E_1-E_4) and peritectic (U_1-U_4) points, the coordinates of which are given in Table 1.

The liquidus shows isothermal lines every 200 K, which control the course of monovariant curves.

The solid-phase equilibria diagram of the Ce_2Se_3-Sb_2Se_3-Bi_2Se_3 quasi-ternary system at 300 K reflects the equilibrium of the solid phase in the subsolidus (Fig. 7).

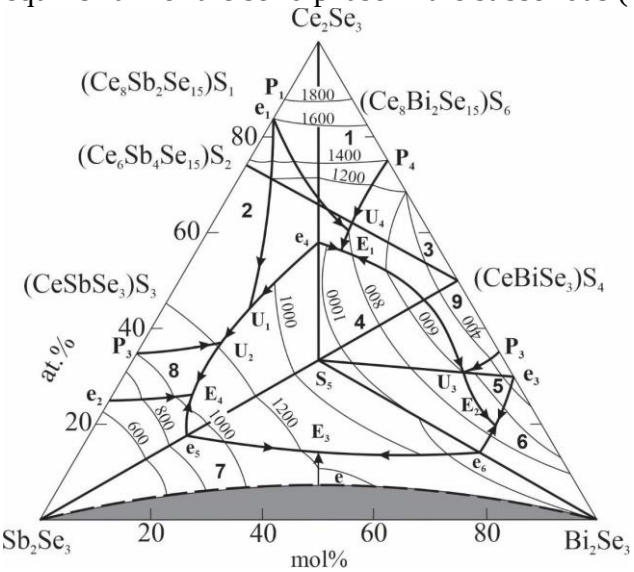

Fig.6. *The projection of the liquidus surface of the Ce_2Se_3-Sb_2Se_3-Bi_2Se_3 quasi-ternary system. Fields of primary crystallization: 1-Ce_2Se_3; 2-S_2; 3-S_6; 4-S_5; 5-S_4; 6-Bi_2Se_3;7- Sb_2Se_3;8-S_3*

Table 1.

Nonvariant equilibria in the Ce_2Se_3-Sb_2Se_3-Bi_2Se_3 quasi-ternary system

Point on the Fig.6	***Equilibria***	***Temperature, K***
E_1	$L \leftrightarrow Ce_2Se_3 + S_5 + S_4$	605
E_2	$L \leftrightarrow S_5 + S_4 + Bi_2Se_3$	710
E_3	$L \leftrightarrow S_5 + Sb_2Se_3 + Bi_2Se_3$	748
E_4	$L \leftrightarrow Sb_2Se_3 + S_5 + Ce_2Se_3$	497
U_1	$L + S_1 \leftrightarrow U_1 + S_5$	704
U_2	$L + S_2 \leftrightarrow U_2 + S_5$	598
U_3	$L + S_4 \leftrightarrow U_3 + S_5$	806
U_4	$L + Ce_2Se_3 \leftrightarrow U_4 + S_4$	783

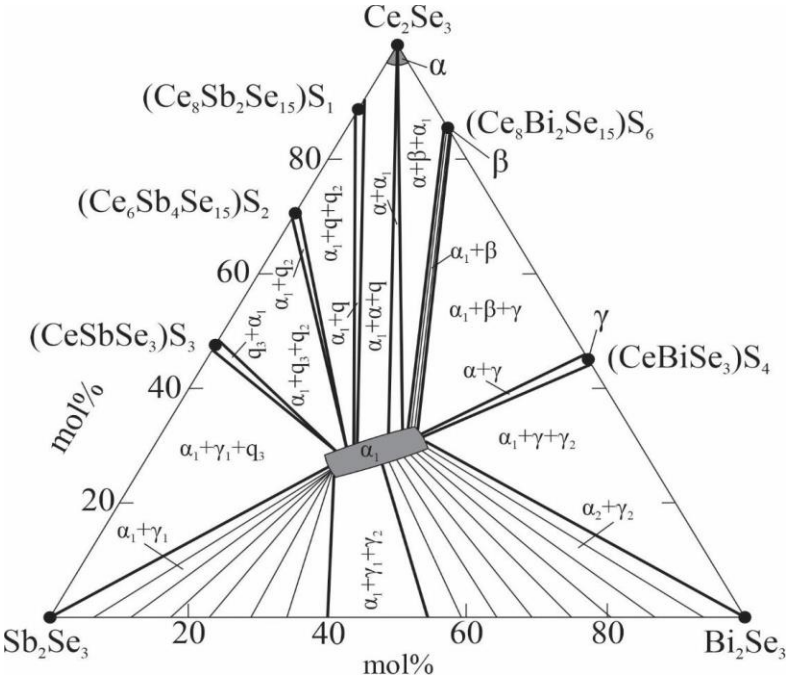

Fig.7. *Isothermal section of the Ce_2Se_3-Sb_2Se_3-Bi_2Se_3quasi-ternary system. q_1 (S_1), q_2(S_2), q_3 (S_3),α_1 (S_5 əsasında bərk faza), α (Ce_2Se_3 əsasında bərk faza)*

As can be seen from Fig. 7, the subsolidus of the ternary system consists of 16 fields of primary crystallization, of which 8 are two-phase and 8 are three-phase regions.

CONCLUSIONS

Based on the set of the obtained experimental results and literature data, the character of phase equilibria in the Ce_2Se_3-Sb_2Se_3-Bi_2Se_3 quasi-ternary system has been established. Phase diagrams of a number of internal cross sections, an isothermal cross section at 300 K, and projections of the liquidus surface are constructed, and the types and coordinates of non and monovariant equilibria are established. The data obtained can be used to select the compositions of alloys during directional crystallization from the melt.

REFERENCES

1. Baghbanzadeh-Dezfuli B., Jamali-Sheini F., Cheraghizade M. Sonical deposition of nanostructured Sb_2Se_3 films for optoelectronic applications // Journal of Alloys and Compounds, 2021, v.25, p. 157308
2. Wang F,K., Yang S.J., Zhai T.Y. 2D Bi_2Se_3 materials for optoelectronics // IScience, 2021, v.24, Issue 11, p.103291
3. Ghosh S., Moreira M.V.B., Fantini C., González J.C. Growth and optical properties of nanocrystalline Sb_2Se_3 thin-films for the application in solar-cells // Solar Energy, 2020, v. 211, p.613-621
4. Venkatasubramanian R., Siivola E., Colpitts T., O'Quinn B. Thin-film thermoelectric devices with high room-temperature figures of merit // Nature, 2001, v.413, p.597-602
5. An D., Chen S., Lu Z., Li R., Chen W., Fan W., Wang W, and Wu Y. Low Thermal Conductivity and Optimized Thermoelectric Properties of p-Type Te–Sb_2Se_3: Synergistic Effect of Doping and Defect Engineering // CS Appl. Mater. Interfaces, 2019, v.11, No31,

p.27788–27797
6. Wu J-K, Hofmann M., Hsieh W-P, Chen S-H, Yen Z-L., Chiu S-K., Luo Y-R., Chiang C-C, Huang Y., Huang S-Y., Chang Y-H., and Hsieh Y-P. Enhancing Thermoelectric Properties of 2D Bi_2Se_3 by 1D Texturing with Graphene // ACS Appl. Energy Mater. 2019, v.2, No.12, p.8411–8415
7. Kim H.C., Oh T.S., Hyun D.B. Thermoelectric properties of the p-type Bi_2Te_3-Sb_2Te_3-Sb_2Se_3 alloys fabricated by mechanical alloying and hot pressing. // Journal of Physics and Chemistry of Solids, 2000, v.61(5), p.743-749
8. Yang, W., Kim, J.H., Hutter, O.S. et al. Benchmark performance of low-cost Sb_2Se_3 photocathodes for unassisted solar overall water splitting. // Nature Communications, 2020, v. 11, p.861
9. Sankapal B.R., Lokhande C.D. Studies on photoelectrochemical (PEC) cell formed with SILAR deposited Bi_2Se_3-Sb_2Se_3 multilayer thin films. // Sol. Energy Mater. Sol. Cell. 2001, v. 69, p.43-52.
10. Li W., Deng L., Wang X., Cao J., Xie Y., Zhang Q., Zhang H., Deng H. and Cheng S. Close-spaced thermally evaporated 3D Sb_2Se_3 film for high-rate and high-capacity lithium-ion storage // Nanoscale, 2021, v.13, p.9834-9842
11. Xue M.-Z., Fu Z.-W. Pulsed laser deposited Sb_2Se_3 anode for lithium-ion batteries // J. Alloys and Compounds, 2008, v.458. p.351-356
12. Ma J., Wang Y., Wang Y., Chen Q., Lian J., Zheng W., Controlled synthesis of one-dimensional Sb_2Se_3 nanostructures and their electrochemical properties // J. Phys. Chem. C, 2009, v. 113, p.13588-13592
13. Zhang H., Liu C.-X., Qi X.-L., Dai X., Fang Z., Zhang S.-C. Topological insulators in Bi_2Se_3, Bi_2Te_3 and Sb_2Te_3 with a single Dirac cone on the surface // Nat. Phys., 2009, v. 5, p.438.
14. Mazumder K., Shirage P.M. A brief review of Bi_2Se_3 based topological insulator: From fundamentals to applications // Journal of Alloys and Compounds, 2021, v.888, p. 161492
15. Anversa J. Chakraborty S., Piquini P., Ahuja R. High pressure driven superconducting critical temperature tuning in Sb_2Se_3 topological insulator // Appl. Phys. Lett., 2016, v. 108, p.212601.
16. Kong P.P., Sun F., Xing L.Y., Zhu J., Zhang S.J., Li W.M., Liu Q.Q., Wang X.C., Feng S.M. et al. Superconductivity in strong spin orbital coupling compound Sb_2Se_3 // Sci. Rep., 2014, No4, p. 6679
17. Шурова М.А, Андреев О.В, Харитонцев В.Б. Фазовые равновесия в системе Bi_2Se_3-Sm_2Se_3 // Вестник Тюменского Государственного Университета. Социально-экономические и правовые исследования, 2014, N5, с.113-121
18. Andreev O.V., Kharitsontsev V.B., Elyshev A.V. Compositions of phrases in the interaction of rare-earth metals with selenium// Russ J.Inorg.Chem., 2013, v.58, p.910
19. Мамедова С.Г., Садыгов Ф.М., Гасымов В.А. и др. Исследование систем Sb_2Se_3-CeSe и Bi_2Se_3-CeSe / Ж. Неорг. Химии, 2003, т.48, N3, с.494-496
20. Садыгов Ф.М., Мамедова С.Г., Бабанлы М.Б., Ильяслы Т.М. Фазовые равновесия в системе Ce-Sb-Se по разрезу Sb_2Se_3-Ce_2Se_3 // Журн. Неорг. химии, 2001, т.46, N8, с.1382-1383
21. Ганбарова Г.Т., Садыгов Ф.М., Гасымов В.А., Исмаилов З.И. и др. Исследование химического взаимодействия в системе Sb_2Se_3-NdSe// J.Qafqaz University Chemistry and Biology, 2013, т.1, N2, с.158-160
22. Садыгов Ф.М., Джафарова Е.К., Бабанлы М.Б. и др. Взаимодействие в тройной системе Tm-Bi-Se по разрезам Bi_2Se_3- Tm_2Se_3 и Bi_2Se_3- Tm_3Se_4 // Журн. Неорг. химии, 2001, т.46,

N8, c.1379-1381
23. Садыгов Ф.М., Джафарова Е.К., Бабанлы М.Б. и др. Характер фазообразования в системах Sb_2Se_3 (Bi_2Se_3)- TmSe // Журн. Неорг. химии, 2002, т.47, N10, с.1713
24. Садыгов Ф.М., Ильяслы Т.М., Насибова Л.Э., Алиев И.И. Физико-химическое исследование системы Sb_2Se_3-Nd_2Se_3// Журн. Неорг. химии, 2013, т.58, N9, с.1253-1256.
25. Садыгов Ф.М., Ильяслы Т.М., Ганбарова Г.Т., Зломанов В.П., Алиев И.И. Физико-химическое исследование системы Sb_2Se_3-Nd_2Se_3 // Неорг.Матер.2017, т.53, N7, с.681-685.
26. Sadigov F.M., Ganbarova G.T., İlyasly T.M., İsmayilov Z.İ., Shukurova G.M., Mammadova S.H. Character of Chemical İnteractions on Bi_2Se_3-Nd_2Se_3 section in Nd-Bi-Se system // J. National Science Review, 2017, v.4, p.1266-1275
27. Абдулсалямова М.Н., Физикохимия антимонидов и висмутидов редкоземельных элементов, Журнал Всесоюзного Химического Общества, О.И.Менделеева, 1981т.XXVI, №6, , с. 73-78
28. Лякишев, Р.П. Диаграммы состояния двойных металлических систем / Р.П.Лякишев. Москва: Машиностроение, Справочник, - т.1.- 1996.- 992с; - т.2.- 1997. –1024 с; т.3.-2001. - 872 с.
29. Binary alloy phase diagrams / ed. T.B.Massalski. - second edition. - ASM International, Materials Park, - Ohio, v.3. - 1990. -3589 p.

XÜLASƏ

S.H.Məmmədova, F.M.Sadıqov

Ce_2Se_3-Sb_2Se_3-Bi_2Se_3 KVAZİÜÇLÜ SİSTEMİNDƏ FAZAƏMƏLƏGƏLMƏ

Ədəbiyyat məlumatları və fiziki-kimyəvi analiz üsullarının nəticələrinə əsasən, Ce_2Se_3-Sb_2Se_3-Bi_2Se_3 kvaziüçlü sistemində fazaəmələgəlmənin xarakteri müəyyən edilmişdir. Bir sıra daxili kəsiklərin (Sb_2Se_3-$CeBiSe_3$, Ce_2Se_3-$CeSb_{1,5}Bi_{1,5}Se_6$, Bi_2Se_3-$CeSb_{1,5}Bi_{1,5}Se_6$, $CeSbSe_3$ - $CeBiSe_3$) hal diaqramları, sistemin 300 K-də izotermik kəsiyi, həmçinin likvidus səthinin proüeksiyası qurulmuş, non və monovariant tarazlıqların tipləri və koordinatları təyin edilmişdir. Sistemdə altı üçlü birləşmənin S_1($Ce_8Sb_2Se_{15}$), S_2($Ce_6Sb_4Se_{15}$), S_3($CeSbSe_3$), S_4 ($CeBiSe_3$), S_5($CeSb_{1,5}Bi_{1,5}Se_6$) and S_6 ($Ce_8Bi_2Se_{13}$) mövcud olducu, həmçinin Sb_2Se_3 , Bi_2Se_3 ilkin komponentlər və S_5 birləşməsi əsasında bərk məhlul sahələri aşkar edilmişdir.

Açar sözlər: *Stibium və bismut xalkogenidləri, NTE xalkogenidləri, kvazi-binar kəsik, qeyri-kvazi-binar kəsik, likvidus səthinin proyeksiyası*

РЕЗЮМЕ

Ш.Х.Мамедова, Ф.М.Садыков

ФАЗООБРАЗОВАНИЕ В КВАЗИТРОЙНОЙ СИСТЕМЕ Ce_2Se_3-Sb_2Se_3-Bi_2Se_3

На основании совокупности литературных данных, а также результатов, полученных методами физико-химического анализа, установлен характер фазообразования в квазитройной системе Ce_2Se_3-Sb_2Se_3-Bi_2Se_3. Построены диаграммы состояния ряда внутренних сечений (Sb_2Se_3-$CeBiSe_3$, Ce_2Se_3-$CeSb_{1,5}Bi_{1,5}Se_6$, Bi_2Se_3-$CeSb_{1,5}Bi_{1,5}Se_6$, $CeSbSe_3$ -$CeBiSe_3$), изотермическое сечение при 300 К, а также проекция поверхности ликвидуса, определены типы и координаты нон- и моновариантных равновесий. В системе обнаружено существование шести тройных соединений- S_1($Ce_8Sb_2Se_{15}$), S_2($Ce_6Sb_4Se_{15}$), S_3($CeSbSe_3$), S_4 ($CeBiSe_3$), S_5($CeSb_{1,5}Bi_{1,5}Se_6$) и S_6 ($Ce_8Bi_2Se_{13}$), а также области твердых растворов на основе исходных Sb_2Se_3 , Bi_2Se_3 , а также соединения S_5.

Ключевые слова: *Халькогениды сурьмы и висмута, халькогениды РЗЭ, квазибинарный разрез, неквазибинарный разрез, проекция поверхности ликвидуса*